HYDRATION OF MELT GRAINS FROM THE HIAWATHA CRATER, NORTH-WEST GREENLAND: EVIDENCE FOR IMPACT THROUGH THE GREENLAND ICE SHEET? Adam A. Garde[1], Nynke Keulen[1] and Tod Waight[2]. [1]Geological Survey of Denmark and Greenland (GEUS), Denmark, aag@geus.dk, [2]Department of Geosciences and Natural Resource Management, University of Copenhagen, Denmark.

Introduction: The recently discovered, 31-km wide Hiawatha impact crater in NW Greenland is covered by the Greenland Ice Sheet. Indirect evidence such as disturbance of the lower part of its ice-radar stratigraphy, excessive current meltwater discharge suggesting remanent impact heat and identification of impact-affected conifer charcoal [1, 2], suggests the crater may be very young, but important questions remain. What is the precise age of the crater, and can the impact be correlated with known climatic events? Was an ice sheet aged 2.6 Ma or less [3] present when the impact occurred? Here we present new evidence about the cooling history and hydration of the crater, based on study of impact melt grains hand-picked from glaciofluvial sand draining it.

Analytical methods: Optical microscopy. Scanning electron microscopy with ultrahigh-resolution automated quantitative mineralogy (AQM) applying Zeiss Mineralogic software [4] and backscattered-electron (BSE) imaging. Electron microprobe (EMP-WDS) element mapping. Raman spectrography.

Observations: The impactite grains studied here are clast-free to clast-rich, hypo- to almost holocrystalline melt particles; see [1, 2, 5] for other types of impactite grains. Their microstructures indicate rapid crystallisation in strongly undercooled melts and glasses, high-temperature hydration of felsic glasses and low-temperature hydrothermal alteration. Many grains contain fragments of plagioclase with checkerboard structure and quartz with shock lamellae, proving their impact origin.

Most melt grains are glassy or contain euhedral microlites in a glassy matrix. The grain shown in Fig. 1A has moderate contents of euhedral microlites ~25–75 µm long. The grain in Fig. 1B contains much more abundant, very tiny acicular microlites. The microlites in both grains are interpreted as having crystallised from melts well above the solidus, but at different degrees of undercooling (see discussion). Other melt grains have a hemicrystalline matrix of ternary feldspar with imperfect stoichiometric composition. Still other melt grains consist of highly unusual, closely packed, zoned feldspar spherulites ≤ 50 µm in size (Fig. 2). These grains are also interpreted as having crystallised from melts at strong disequilibrium conditions (see discussion).

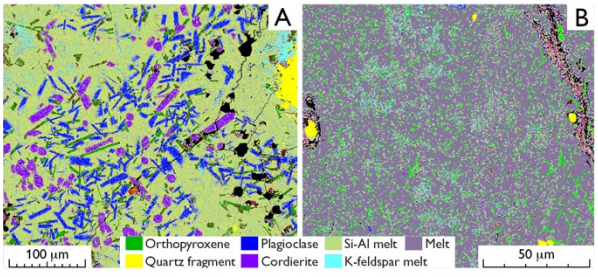


Fig. 1. Quenched melt grains. **A**. Grain 21K-w39 with relatively few, large microlites. **B**. Grain 21D-r06 with abundant, very small microlites. Undercooling prior to full quenching was most pronounced in B, with more nucleation but less crystal growth. SEM-EDS composition maps with indexed mineral and glass phases.

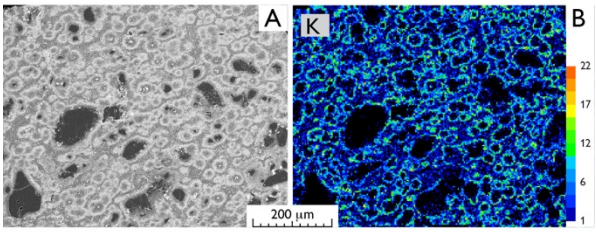


Fig. 2. Zoned feldspar spherulites in grain 21G-d05, nucleated on fragments of quartz. **A**. SEM-BSE image. **B**. EMP-WDS potassium map. K-feldspar spherulite rims (light blue) on plagioclase cores (dark blue), nucleated on quartz (black). Arbitrary scale.

A distinct population of felsic melt grains without microlites records a specific event of hot, near-isochemical hydration. These grains contain abundant perlitic fractures with a spacing of ~100–200 µm (Fig. 3), with interior 'beads' between the curved fractures consisting of closely packed mordenite spherulites just 1–3 µm in size, identified by Raman spectrography (Fig. 3C). An

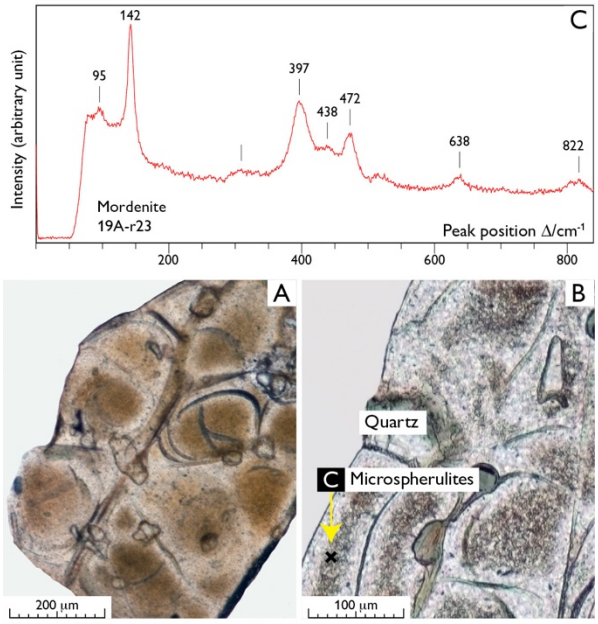


Fig. 3. **A, B**. Optical microphotographs of felsic melt grains 21J-z40 (A) and 19A-r23 (B) with perlitic fracturing, chilled walls and mordenite microspherulites in ovoid melt interiors. **C**. Raman spectrum of mordenite in grain 19A-r23 with automatically indexed peak positions using WiTec software Project Four.

absence of spherulites in chilled fracture walls shows that the perlitic fracturing and mordenite microspherulites were contemporaneous. The high-temperature isochemical hydration event was succeeded by a second event of localised, low-temperature, fracture-bound hydrothermal alteration with introduction of K and Fe and removal of Ca and Si along the fractures (Fig. 4).

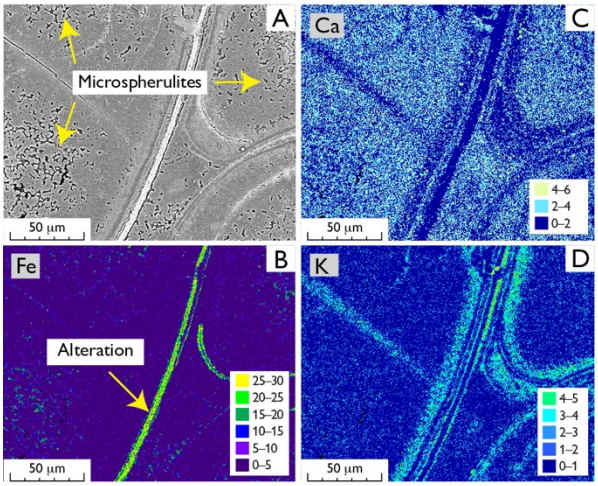


Fig. 4. Microspherulitic mordenite within 'beads' inside perlitic fractures, and younger hydrothermal alteration with Fe and K enrichment and Ca depletion along the fractures in grain 21J-z40 shown in Fig. 3A. **A.** SEM-BSE image. **B–D**. SEM-EDS composition maps of Fe, Ca and K (in element wt%).

Discussion: The microlite-bearing Hiawatha melt grains all contain evidence of high nucleation rates but inhibited diffusion and crystal growth, indicating strong undercooling [6]. This is most obvious in grain 21D-r06 (Fig. 1B) with its abundant, minute microlites. Non-stoichiometric feldspar compositions in grains with hemicrystalline matrix also indicate undercooling and full quenching without maturing recrystallisation.

Melt grains with small, closely packed, zoned feldspar spherulites only tens of micrometres in size (Fig. 2) are extremely unusual both in terrestrial and impact melt rocks. By analogy with a rare occurrence of feldspar-spherulitic, contact-melted arkosic rocks adjacent to Tertiary intrusions on the Isle of Rum, U.K. [7] they most likely crystallised from strongly undercooled melts close to the solidus, in a setting where element diffusion and spherulite growth in the melt may have been enhanced by uptake of H_2O.

The perlitic melt grains packed with mordenite might be still more significant. The perlitic fracturing and mordenite growth were simultaneous and occurred within the stability field of mordenite, in a setting with access to clean hydrous fluid/vapour. The subsequent low-temperature, fracture-bound hydrothermal alteration recorded in the same grains resembles meteoric alteration systems found in many impact craters. Perlitic fracturing as such is a common phenomenon in rhyolites and normally occurs at low temperatures < 200°C [8], whereas mordenite belongs to the high-temperature end of the zeolite group, with an estimated stability field of ~ 250–400°C and typically found in cavities of altered mafic volcanic rocks or as secondary replacement in low-grade metamorphic pyroclastic rocks [9, 10]. However, an exceptional occurrence of syneruptive mordenite and heulandite associated with intense perlitic fracturing has been described from recent, subglacial rhyolites in southern Iceland [11], where it was concluded that the fracturing and zeolite growth were driven by ingress of glacial water vapour from the adjacent and overlying glacier [11].

The Hiawatha mordenite microspherulite crystallisation must have occurred during post-impact cooling of the crater but prior to the fracture-bound alteration with meteoric H_2O. This suggests rapid crater infilling by a clean hydrous source before the meteoric hydrothermal stage. Meltwater from an ice sheet surrounding the hot crater would constitute a perfect source for this.

Conclusions: The many different Hiawatha melt grains reflect incomplete crystallization at different temperatures and degrees of undercooling. The highly unusual perlitic grains most closely resemble subglacially erupted mordenite- and heulandite-bearing perlitic rhyolites in South Iceland and document a very specific hydration event during post-impact cooling, presumably at 250–400°C [9, 11]. An influx of water was required – not immediately after the initial cratering as in a submarine impact, but a little later in the cooling history and prior to low-temperature hydrothermal circulation of meteoric water. An adequate source of H_2O must have become available at this point, which suggests that the target area was glaciated when the impact occurred – in agreement with previously reported indirect evidence that the Hiawatha crater may be very young.

Acknowledgements: We thank Pierre Beck (Univ. Grenoble, France) and Troels Nielsen (GEUS, Denmark) for for discussion, and Lisbeth Garbrecht Thygesen (Univ. Copenhagen, Denmark) for assistance with Raman spectrography.

References: [1] Kjær K. H. et al. (2018) *Science Advances,* 4, eaar8173. [2] Garde A. A. et al. (2020) *Geology*, 48, 867–871. [3] Biermann P. R. et al. (2016) *Nature*, 540, 256–260. [4] Graham S. & Keulen N. (2019) *Minerals*, 9, 665. [5] Hyde W. R. et al. (*LPSC abstract, this conference.* [6] Best M. G. (2003) Igneous and Metamorphic Petrology. Oxford: Blackwell. [7] Holness M. B. (2002) *Geol. Magazine*, 139, 651–663. [8] Bindemann H. N. & Lowenstern J. B. (2016) *Contrib. Min. Pet.,* 171:79. [9] Pe-Piper G. (2002) *Canadian Mineral.,* 38, 1215–1232. [10] Ghiara M. R. et al. (1999) *Clays and Clay Minerals*, 47, 319–328. [11] Denton J. S. et al. (2009) *J. Geol. Soc., London*, 166, 895–904.